Research

Author for correspondence:

R.M. Potvliege
e-mail: r.m.potvliege@durham.ac.uk

Non-Hermitian Floquet dynamics in absorption spectroscopy

R. M. Potvliege

Department of Physics, Durham University, Durham DH1 3LE, UK

RP, 0000-0003-4624-1064

A theory of the absorption of a laser field by an atomic or condensed matter medium is presented for the case where the medium is also interacting with a strong electromagnetic field. The rotating wave approximation is not assumed for the latter. It is shown that in the weak probe limit the Lindblad master equation reduces to a smaller system of linear equations for the relevant steady-state coherences. In this limit, the complex susceptibility of the medium can be expressed in terms of individual contributions of decaying dressed states, the latter being eigenstates of a non-Hermitian Floquet Hamiltonian.

1. Introduction

This article primarily concerns the theory of the absorption of a weak laser beam by an atomic or condensed matter medium driven by one or several other electromagnetic fields. It specifically focuses on the case where at least one of these fields is too strong to be considered within the rotating wave approximation. Typically, this strong field would be a microwave or radio frequency field, though the theory is not confined to these scenarios. The relevance of the Floquet theory of linear differential equations with periodic coefficients has long been recognized in this context and in other areas of quantum optics [1–3]. Its relevance is easily appreciated from the fact that the Hamiltonian describing the interaction of a quantum system with a continuous-wave monochromatic electromagnetic field is periodic in time, assuming no other time-dependent interactions. However, the theory also applies to stationary multi-frequency fields [4–6] and helps in understanding the dynamics of quantum systems interacting with

non-stationary fields, e.g. the dynamics of atoms in intense laser pulses [7–9]. In more recent years, Floquet theory has considerably expanded into the rapidly developing field of Floquet engineering, which aims at using period interactions for generating and controlling new states of complex quantum systems—e.g. [10–21] and references therein. The relationship between the quantum and classical Floquet formalisms has been recently clarified in [21], which also offers a new general formalism for the modelling of driven open quantum systems.

A full Floquet description is often unnecessary for the relatively weak, near-resonant fields typically used in spectroscopic measurements. The rotating wave approximation can usually be made for such fields, which simplifies the theory considerably [6,22]. However, this approximation is not always justified. For example, going beyond the rotating wave approximation is normally essential in applications of Floquet theory to the modelling of multiphoton ionization and other multiphoton processes driven by a strong laser field [5–7,9,23,24], to the measurement of low-frequency fields using atoms in Rydberg states [25–29], and of course for understanding how the properties of atomic or other systems can be manipulated through Floquet engineering.

Floquet calculations involve replacing the time-dependent Hamiltonian of the system of interest with a time-independent Hamiltonian acting in a larger Hilbert space, the 'Floquet Hamiltonian' [1,2]. This Floquet Hamiltonian is non-Hermitian in some cases, for example, in the cases considered in [30] or in [31]. In particular, it is non-Hermitian in the complex dilation approach to multiphoton ionization in a strong laser field [23,24]: the radial variable r is replaced by $r \exp(i\theta_r)$ for a well-chosen value of the angle θ_r, which transforms the Floquet Hamiltonian into a non-Hermitian operator. Doing so yields complex quasienergies the imaginary parts of which within a factor of $(-2/\hbar)$, give the ionization rates of the states of interest [32]. This approach to multiphoton ionization is mathematically rigorous [33–35]. The Floquet Hamiltonian is also non-Hermitian for the systems we are studying in this work, but for a different reason.

The present theory concerns the absorption of a weak beam by a medium modelled as an ensemble of individual systems with a finite number of bound energy eigenstates, for the case where some of these bound states may decay radiatively or otherwise. For instance, the methods outlined below have recently been applied to the calculation of the absorption of a weak probe beam by a cuprous oxide (Cu_2O) sample driven by a strong microwave field [36]. In this system, the probe beam couples the valence band (treated as a single bound state) to broad Rydberg excitons decaying through interaction with phonons. These methods could also be applied to the spectroscopy of a strongly driven atomic vapour in which excited atoms decay radiatively. The quantum state of such media can usually be described by a density matrix satisfying the Lindblad master equation. Floquet approaches to this problem have been discussed in the literature—see, e.g. [37–40] and, in regard to the optical properties of the medium, [41–47]. However, and as we show in this article, a full Lindblad-Floquet calculation is not necessary in the weak probe limit, i.e. in the quite common case where the probe field is weak enough to be treated in first order of perturbation theory. Indeed, the master equation reduces in this case to a set of simpler equations where each decaying bound state is associated with a complex energy: i.e. the real energies $\hbar\omega^{(i)}$, $i = 0, 1, 2, ...$, of the different states included in the model are replaced by the complex energies $\hbar\omega^{(i)} - i\hbar\Gamma^{(i)}/2$, $i = 0, 1, 2, ...$, where $\Gamma^{(i)}$ is the decay rate of state i. The properties of the medium can then be described in terms of the eigenstates of a non-Hermitian Floquet Hamiltonian, this Hamiltonian being non-Hermitian because of the non-zero imaginary parts of these complex energies. In particular, the calculation yields the linear susceptibility of the medium as a sum of contributions from the decaying dressed states of the Floquet Hamiltonian. We stress that the imaginary parts of these energies are rigorously derived from the master equation, here, and are not ad hoc additional phenomenological decay widths.

For simplicity, this article only considers the case of a homogeneous single species medium interacting with two monochromatic electromagnetic fields, namely, a weak probe field and a strong coupling field, both polarized linearly in the same direction. The theory can be easily generalized to multi-species media and more complex excitation pathways as long as the rotating wave approximation and the Beer-Lambert law apply for the probe field.

3

royalsocietypublishing.org/journal/rspa   *Proc. R. Soc. A* **481**: 20240484

The general theory is developed in §2. Its weak probe, long time limit is discussed in §3. A numerical illustration of the theory is provided in §4.

2. The probe absorption spectrum

(a) The absorption coefficient

As already mentioned, this article primarily concerns experiments in which a strong microwave or some other electromagnetic field (the 'coupling field') is applied to a homogeneous sample addressed by a laser beam (the 'probe field'), in circumstances where the latter is sufficiently weak that its attenuation is well described by the Beer-Lambert law. We thus assume that

$$I(x) = \exp(-Kx)\, I(x = 0), \tag{2.1}$$

where $I(x)$ is the probe intensity at a distance x inside the medium and K, the absorption coefficient, is a constant. For simplicity, we assume that the probe and coupling fields are monochromatic and polarized in the z-direction, that the probe field can be modelled as a plane wave propagating in the x-direction and that the coupling field is homogeneous. We also assume that these fields are turned on at $t = 0$. The details of the turn on are not important in so far as the state of the medium in the $t \to \infty$ limit is concerned, which is the focus of this work. Accordingly, we write their electric field components as follows,

$$\mathbf{E}_\text{p}(x,t) = \frac{1}{2}\, \hat{\mathbf{z}} \left[\mathcal{E}_\text{p}(x) \exp(-i\omega_\text{p} t) + \mathcal{E}_\text{p}^*(x) \exp(i\omega_\text{p} t) \right] H(t), \tag{2.2}$$

$$\mathbf{E}_\text{c}(t) = \frac{1}{2}\, \hat{\mathbf{z}} \left[\mathcal{E}_\text{c} \exp(-i\omega_\text{c} t) + \mathcal{E}_\text{c}^* \exp(i\omega_\text{c} t) \right] H(t), \tag{2.3}$$

where $\hat{\mathbf{z}}$ is a unit vector in the z-direction and $H(t)$ is the Heaviside step function. The probe and coupling fields polarize the medium, resulting in a polarization field $\mathbf{P}(x,t)$. In terms of the density operator $\hat{\rho}(x,t)$ describing the state of the medium at position x and time t,

$$\mathbf{P}(x,t) = N_\text{d} \operatorname{Tr}[\, \hat{\rho}(x,t)\, \hat{D}_z \,]\, \hat{\mathbf{z}}, \tag{2.4}$$

where $\hat{D}_z$ is the z-component of the dipole operator and N_d is the number density of atoms or other individual systems the state of which is described by $\hat{\rho}(x,t)$. Assuming that t is large enough for the medium to have evolved into a stationary state,

$$\mathbf{P}(x,t) = \frac{1}{2}\, \hat{\mathbf{z}} \left[\mathcal{P}_\text{p}(x) \exp(-i\omega_\text{p} t) + \mathcal{P}_\text{p}^*(x) \exp(i\omega_\text{p} t) + \ldots \right], \tag{2.5}$$

where ... stands for contributions oscillating at angular frequencies other than ω_p. The complex polarization amplitude $\mathcal{P}_\text{p}(x)$ is proportional to $\mathcal{E}_\text{p}(x)$ for the weak probe fields considered here: in terms of a frequency-dependent susceptibility $\chi(\omega_\text{p}, \omega_\text{c}, \mathcal{E}_\text{c})$,

$$\mathcal{P}_\text{p}(x) = \epsilon_0\, \chi(\omega_\text{p}, \omega_\text{c}, \mathcal{E}_\text{c})\, \mathcal{E}_\text{p}(x). \tag{2.6}$$

If it follows from the above [48] that

$$K = 2(\omega_\text{p}/c) \operatorname{Im} \left[1 + \chi(\omega_\text{p}, \omega_\text{c}, \mathcal{E}_\text{c}) \right]^{1/2}. \tag{2.7}$$

The absorption coefficient K does not depend on x since the coupling field is taken to be homogeneous. Accordingly, we no longer specify the spatial dependence of $\mathcal{E}_\text{p}(x)$, $\mathcal{P}_\text{p}(x)$ and $\hat{\rho}(x,t)$.

(b) Microscopic description

We use a finite basis of $\mathcal{N}$ orthonormal eigenstates of the medium's field-free Hamiltonian, $\hat{H}_0$, that is, a basis $\{|i\rangle, i = 0, \ldots, \mathcal{N} - 1\}$ such that $\langle i|j\rangle = \delta_{ij}$ and

$$\hat{H}_0|i\rangle = \hbar\omega^{(i)}|i\rangle, \qquad i = 0, \ldots, \mathcal{N} - 1. \tag{2.8}$$

We describe the interaction between the medium and the applied fields within the electric dipole approximation. The Hamiltonian of the system can, therefore, be written in the following way in terms of the Rabi frequencies $\Omega_{\mathrm{p};ij} = \mathcal{E}_{\mathrm{p}}\langle i|\hat{D}_z|j\rangle/\hbar$ and $\Omega_{\mathrm{c};ij} = \mathcal{E}_{\mathrm{c}}\langle i|\hat{D}_z|j\rangle/\hbar$:

$$\hat{H}(t) = \sum_i \hbar\omega^{(i)}|i\rangle\langle i| - \frac{\hbar}{2}\sum_{i,j}\left\{\left[\Omega_{\mathrm{p};ij}\exp(-i\omega_{\mathrm{p}}t) + \Omega_{\mathrm{c};ij}\exp(-i\omega_{\mathrm{c}}t)\right]|i\rangle\langle j| + \mathrm{h.c.}\right\}. \tag{2.9}$$

Typically, the relevant states form two groups differing considerably in energy, namely, a low-energy group A and a higher-energy group B. We will assume that the coupling field strongly couples the states of group B to each other, but does not directly couple the states of group A to each other or to those of group B, while the probe field only couples states of group A to states of group B. Neglecting the far-detuned transitions, we thus set

$$\hat{H}(t) = \sum_i \hbar\omega^{(i)}|i\rangle\langle i| - \frac{\hbar}{2}\sum_{i\in A}\sum_{j\in B}\left[\Omega_{\mathrm{p};ij}\exp(-i\omega_{\mathrm{p}}t)|i\rangle\langle j| + \mathrm{h.c.}\right]$$

$$- \frac{\hbar}{2}\sum_{i\in B}\sum_{j\in A}\left[\Omega_{\mathrm{p};ij}\exp(-i\omega_{\mathrm{p}}t)|i\rangle\langle j| + \mathrm{h.c.}\right]$$

$$- \frac{\hbar}{2}\sum_{i\in B}\sum_{j\in B}\left[\Omega_{\mathrm{c};ij}\exp(-i\omega_{\mathrm{c}}t)|i\rangle\langle j| + \mathrm{h.c.}\right]. \tag{2.10}$$

Given this Hamiltonian, the density operator $\hat{\rho}(t)$ is governed by the Lindblad master equation

$$\frac{\mathrm{d}\hat{\rho}}{\mathrm{d}t} = -\frac{i}{\hbar}[\hat{H}, \hat{\rho}] + \frac{1}{2}\sum_n\left(2\hat{C}_n\hat{\rho}\hat{C}_n^\dagger - \hat{C}_n^\dagger\hat{C}_n\hat{\rho} - \hat{\rho}\hat{C}_n^\dagger\hat{C}_n\right), \tag{2.11}$$

where the $\hat{C}_n$'s are the collapse (or jump) operators accounting for decoherence and relaxation. The $\hat{C}_n$'s should include the operator $\sqrt{\Gamma_{ij}}|i\rangle\langle j|$ if state j relaxes to state i at a rate Γ_{ij}, e.g. by spontaneous decay.

(c) The rotating wave approximation

We will also assume that the energies are measured with respect to a given reference energy $\hbar\omega^{\mathrm{ref}}$ chosen so that the differences $|\omega^{(i)} - \omega^{\mathrm{ref}}|$ are much smaller for the states of group A than for those of group B. Conversely, the differences $|\omega_{\mathrm{p}} - (\omega^{(i)} - \omega^{\mathrm{ref}})|$ are much smaller for the states of group B than for those of group A. We can thus pass to slowly varying variables by transforming state vectors and density operators by the unitary transformation[1]

$$\hat{U}(t) = \exp\left(i\omega^{\mathrm{ref}}t\right)\sum_{i\in A}|i\rangle\langle i| + \exp\left[i\left(\omega^{\mathrm{ref}} + \omega_{\mathrm{p}}\right)t\right]\sum_{j\in B}|j\rangle\langle j|. \tag{2.12}$$

In particular, the operator $\hat{U}(t)$ transforms $\hat{\rho}(t)$ into the density operator

$$\hat{\rho}^{\mathrm{tr}}(t) = \hat{U}(t)\hat{\rho}(t)\hat{U}^\dagger(t), \tag{2.13}$$

and

$$\langle i|\hat{\rho}(t)|j\rangle = \begin{cases} \langle i|\hat{\rho}^{\mathrm{tr}}(t)|j\rangle & \text{if } i \text{ and } j \in A, \\ \exp(i\omega_{\mathrm{p}}t)\langle i|\hat{\rho}^{\mathrm{tr}}(t)|j\rangle & \text{if } i \in A \text{ and } j \in B, \\ \exp(-i\omega_{\mathrm{p}}t)\langle i|\hat{\rho}^{\mathrm{tr}}(t)|j\rangle & \text{if } i \in B \text{ and } j \in A, \\ \langle i|\hat{\rho}^{\mathrm{tr}}(t)|j\rangle & \text{if } i \text{ and } j \in B. \end{cases} \tag{2.14}$$

A short calculation shows that $\hat{\rho}^{\text{tr}}(t)$ evolves in time according to the equation

$$\frac{d\hat{\rho}^{\text{tr}}}{dt} = -\frac{i}{\hbar}[\hat{H}^{\text{tr}}, \hat{\rho}^{\text{tr}}] + \frac{1}{2}\sum_n \left(2\,\hat{C}_n\hat{\rho}^{\text{tr}}\hat{C}_n^\dagger - \hat{C}_n^\dagger\hat{C}_n\hat{\rho}^{\text{tr}} - \hat{\rho}^{\text{tr}}\hat{C}_n^\dagger\hat{C}_n\right), \tag{2.15}$$

where

$$\hat{H}^{\text{tr}}(t) = \hbar\sum_{i\in A}\delta\omega^{(i)}|i\rangle\langle i| - \hbar\sum_{i\in B}\Delta_{\text{p}}^{(i)}|i\rangle\langle i| - \frac{\hbar}{2}\sum_{i\in B}\sum_{j\in A}\left(\Omega_{\text{p};ij}|i\rangle\langle j| + \text{h.c.}\right)$$

$$- \frac{\hbar}{2}\sum_{i\in A}\sum_{j\in B}\left[\Omega_{\text{p};ij}\exp(-2i\omega_{\text{p}}t)|i\rangle\langle j| + \text{h.c.}\right]$$

$$- \frac{\hbar}{2}\sum_{i\in B}\sum_{j\in B}\left[\Omega_{\text{c};ij}\exp(-i\omega_{\text{c}}t)|i\rangle\langle j| + \text{h.c.}\right], \tag{2.16}$$

with $\delta\omega^{(i)} = \omega^{(i)} - \omega^{\text{ref}}$ and $\Delta_{\text{p}}^{(i)} = \omega_{\text{p}} - (\omega^{(i)} - \omega^{\text{ref}})$.

We now make the rotating wave approximation for the probe field, which is to neglect the rapidly oscillating terms in $\exp(\pm 2i\omega_{\text{p}}t)$ appearing in equation (2.16). Accordingly, we set

$$\hat{\rho}(t) = \hat{U}^\dagger(t)\hat{\rho}^{\text{rw}}(t)\hat{U}(t), \tag{2.17}$$

where $\hat{\rho}^{\text{rw}}(t)$ satisfies the equation

$$\frac{d\hat{\rho}^{\text{rw}}}{dt} = -\frac{i}{\hbar}[\hat{H}^{\text{rw}}, \hat{\rho}^{\text{rw}}] + \frac{1}{2}\sum_n \left(2\,\hat{C}_n\hat{\rho}^{\text{rw}}\hat{C}_n^\dagger - \hat{C}_n^\dagger\hat{C}_n\hat{\rho}^{\text{rw}} - \hat{\rho}^{\text{rw}}\hat{C}_n^\dagger\hat{C}_n\right), \tag{2.18}$$

with

$$\hat{H}^{\text{rw}}(t) = \hbar\sum_{i\in A}\delta\omega^{(i)}|i\rangle\langle i| - \hbar\sum_{i\in B}\Delta_{\text{p}}^{(i)}|i\rangle\langle i| - \frac{\hbar}{2}\sum_{i\in B}\sum_{j\in A}\left(\Omega_{\text{p};ij}|i\rangle\langle j| + \text{h.c.}\right)$$

$$- \frac{\hbar}{2}\sum_{i\in B}\sum_{j\in B}\left[\Omega_{\text{c};ij}\exp(-i\omega_{\text{c}}t)|i\rangle\langle j| + \text{h.c.}\right]. \tag{2.19}$$

The density operator $\hat{\rho}^{\text{rw}}(t)$ is represented by the matrix $[\rho_{ij}^{\text{rw}}(t)]$ in the basis $\{|0\rangle, \ldots, |\mathcal{N}-1\rangle\}$, with

$$\rho_{ij}^{\text{rw}}(t) = \langle i|\hat{\rho}^{\text{rw}}(t)|j\rangle. \tag{2.20}$$

Arranging the matrix elements $\rho_{ij}^{\text{rw}}(t)$ into a column vector $\mathsf{r}(t)$ makes it possible to recast equation (2.18) into a more standard form, that is,

$$\frac{d\mathsf{r}}{dt} = \mathsf{L}(t)\mathsf{r}(t), \tag{2.21}$$

where $\mathsf{L}(t)$ is a $\mathcal{N}^2 \times \mathcal{N}^2$ matrix.

(d) Floquet formulation

In principle, calculating the absorption coefficient reduces to solving equation (2.18) or equation (2.21), calculating the resulting polarization field $\mathbf{P}(x, t)$ and obtaining the polarization amplitude $\mathcal{P}_{\text{p}}(x)$ by Fourier-transforming $\mathbf{P}(x, t)$. As will become clear later on, however, there are advantages to first calculating the Fourier components of the density operator, and thereby seek solutions of the Lindblad master equation in the Floquet form. We note, in this regard, that $\mathsf{L}(t)$ can be written in terms of three constant matrices, L_0, L_+ and L_-, in the following way:

$$\mathsf{L}(t) = \mathsf{L}_0 + \exp(i\omega_{\text{c}}t)\mathsf{L}_- + \exp(-i\omega_{\text{c}}t)\mathsf{L}_+. \tag{2.22}$$

The time-periodicity of $\mathsf{L}(t)$ suggests we seek a solution of equation (2.21) of the form

$$\mathsf{r}(t) = \sum_N \exp(-iN\omega_{\text{c}}t)\mathsf{r}_N(t), \tag{2.23}$$

the $r_N(t)$ being time-dependent column vectors such that

$$\frac{\mathrm{d}r_N}{\mathrm{d}t} = A_N r_N(t) + L_+ r_{N-1}(t) + L_- r_{N+1}(t), \quad N = 0, \pm 1, \pm 2, \ldots, \tag{2.24}$$

where $A_N = L_0 + iN\omega_c I$ with I denoting the $\mathcal{N}^2 \times \mathcal{N}^2$ unit matrix. In practice, this infinite system can be truncated to a finite number of equations and the index N restricted to a certain interval $[N_{\min}, N_{\max}]$. Equation (2.24) can be expressed in matrix form as

$$\frac{\mathrm{d}}{\mathrm{d}t} \begin{pmatrix} \vdots \\ r_{-2}(t) \\ r_{-1}(t) \\ r_0(t) \\ r_1(t) \\ r_2(t) \\ \vdots \end{pmatrix} = \begin{pmatrix} \ddots & & & & & \vdots & \\ L_+ & A_{-2} & L_- & & & & \\ & L_+ & A_{-1} & L_- & & & \\ & & L_+ & A_0 & L_- & & \\ & & & L_+ & A_1 & L_- & \\ & & & & L_+ & A_2 & L_- \\ & & \vdots & & & & \ddots \end{pmatrix} \begin{pmatrix} \vdots \\ r_{-2}(t) \\ r_{-1}(t) \\ r_0(t) \\ r_1(t) \\ r_2(t) \\ \vdots \end{pmatrix}, \tag{2.25}$$

or, in a more compact notation, as

$$\frac{\mathrm{d}r}{\mathrm{d}t} = MR(t). \tag{2.26}$$

Apart from the truncation of the Fourier expansion to a finite number of harmonic components, calculating the density matrix through this last equation and equation (2.23) is equivalent to solving the Lindblad equation (2.18). These two approaches produce numerically different results for finite values of $N_{\min}$ and $N_{\max}$; however, and as illustrated by an example in §4, these differences can be made arbitrarily small by taking the interval $[N_{\min}, N_{\max}]$ wide enough.

The density matrix describing the state of the medium can therefore be obtained in terms of the eigenvalues and eigenvectors of the non-Hermitian constant matrix M, unless this matrix is defective. Let us denote the eigenvalues of M by $w^{(k)}$, its right-hand side eigenvectors by $c^{(k)}$ and its left-hand side eigenvectors by $d^{(k)}$, so that $Mc^{(k)} = w^{(k)}c^{(k)}$ and $d^{(k)\dagger}M = w^{(k)}d^{(k)\dagger}$ (the $c^{(k)}$'s and the $d^{(k)}$'s are column vectors). Assuming that these eigenvectors form a basis and are bi-orthogonal (i.e. that $d^{(k)\dagger}c^{(k')} = 0$ if $k \neq k'$),

$$R(t) = \sum_k \alpha_k c^{(k)} \exp\left(w^{(k)}t\right), \tag{2.27}$$

with

$$\alpha_k = \frac{d^{(k)\dagger}R(t=0)}{d^{(k)\dagger}c^{(k)}}. \tag{2.28}$$

Note that, the right-hand side eigenvectors of M define solutions of equation (2.21) in the Floquet form, that is,

$$r(t) = \exp\left(w^{(k)}t\right) \sum_N \exp(-iN\omega_c t)c_N^{(k)}. \tag{2.29}$$

The eigenvectors for which $w^{(k)} = 0$ may describe steady states of the system, i.e. states for which $\mathrm{d}r_N/\mathrm{d}t = 0$. However, the solutions with $w^{(k)} \neq 0$ do not correspond to density operators of constant unit trace and therefore do not represent physically meaningful quantum states.

Since the column vector $r(t)$ is formed by the matrix elements $\rho_{ij}^{\mathrm{rw}}(t)$, the elements of the vectors $r_N(t)$ are the functions $\rho_{ij;N}^{\mathrm{rw}}(t)$ such that

$$\rho_{ij}^{\mathrm{rw}}(t) = \sum_N \exp(-iN\omega_c t)\rho_{ij;N}^{\mathrm{rw}}(t). \tag{2.30}$$

As will be illustrated by a numerical example in §4, the functions $\rho_{ij;N}^{\mathrm{rw}}(t)$ normally converge to constant values in the $t \to \infty$ limit. In the ensuing steady state, the density matrix contains terms

oscillating at the angular frequencies ω_p, $\omega_p \pm \omega_c$, $\omega_p \pm 2\omega_c$, etc. Only the terms oscillating at the angular frequency ω_p contribute to the complex polarization amplitude $\mathcal{P}_p(x)$. Combining equations (2.4)–(2.6), (2.12), (2.17) and (2.30) yields

$$\chi(\omega_p, \omega_c, \mathcal{E}_c) = \frac{N_d}{\epsilon_0 \mathcal{E}_p} \sum_{i \in B} \sum_{j \in A} \langle j | \hat{D}_z | i \rangle \rho_{ij;N=0}^{rw}(t \to \infty). \tag{2.31}$$

Having calculated $\chi(\omega_p, \omega_c, \mathcal{E}_c)$, the probe absorption spectrum can then be deduced from equation (2.7).

Note that, the advantage of the Floquet approach, in this context, is to yield the $N = 0$ harmonic component of the relevant coherences directly. Merely calculating time-dependent populations and coherences is likely to be more conveniently done by solving equation (2.18) than by solving equation (2.26). The Floquet approach has marked advantages for calculations in the weak probe limit, however, as we now discuss.

3. The weak probe limit

(a) General theory

It is often the case, in experiments, that the medium can be taken to be initially in its ground state or in an incoherent superposition of low energy states, and that the probe laser is too weak for producing significant optical pumping over the relevant time scales. This common situation can be modelled by assuming: (i) that the probe field is weak enough that $\hat{\rho}^{rw}(t)$ only needs to be calculated to first order in $\mathcal{E}_p$, and (ii) that the states of group B are initially unpopulated. The latter implies that $\rho_{ij}^{rw}(t) = 0$ at $t = 0$ if state i or state j belongs to group B and that

$$\sum_{i \in A} \rho_{ii}^{rw}(t = 0) = 1. \tag{3.1}$$

We will further assume that $\rho_{ij}^{rw}(t = 0) = 0$ for $j \neq i$ and $\Gamma_{ij} = 0$ if states i and j both belong to group A, which is normally the case in applications. The density operator $\hat{\rho}^{rw}(t)$ reduces to a density operator $\hat{\rho}^{wp}(t)$ in this weak probe approximation:

$$\rho_{ij}^{rw}(t) \approx \rho_{ij}^{wp}(t), \tag{3.2}$$

with $\rho_{ij}^{wp}(t = 0) = \rho_{ij}^{rw}(t = 0)$. One finds, after a straightforward calculation, that

$$\frac{d\rho_{ij}^{wp}}{dt} = 0 \tag{3.3}$$

if state i and state j both belong to group A or both belong to group B, and that

$$\frac{d\rho_{ij}^{wp}}{dt} = i[\omega^{(j)} + \omega_p - \omega^{(i)} + i\Gamma^{(i)}/2]\rho_{ij}^{wp}(t) + \frac{i}{2}\,\Omega_{p;ij}\rho_{jj}^{wp}(t)$$

$$+ \frac{i}{2}\sum_{l \in B}[\Omega_{c;il}\exp(-i\omega_c t) + \Omega_{c;li}^*\exp(i\omega_c t)]\rho_{lj}^{wp}(t) \tag{3.4}$$

if $i \in B$ and $j \in A$. In this last equation, $\Gamma^{(i)}$ denotes the total decay rate of state i:

$$\Gamma^{(i)} = \sum_{n} \Gamma_{ni}. \tag{3.5}$$

In view of equation (2.31), our main aim is to solve equation (3.4) in the long time limit. Proceeding as above, we seek a solution of equation (3.4) of the form

$$\rho_{ij}^{wp}(t) = \sum_{N} \exp(-iN\omega_c t)\rho_{ij;N}^{wp}(t), \tag{3.6}$$

with

$$\frac{d\rho_{ij;N}^{wp}}{dt} = i[\omega^{(j)} + \omega_p - \omega^{(i)} + i\Gamma^{(i)}/2 + N\omega_c]\rho_{ij;N}^{wp}(t) + \frac{i}{2}\,\Omega_{p;ij}\rho_{jj;N}^{wp}(t)$$
$$+ \frac{i}{2}\sum_{l\in B}[\Omega_{c;il}\rho_{lj;N-1}^{wp}(t) + \Omega_{c;li}^{*}\rho_{lj;N+1}^{wp}(t)]. \tag{3.7}$$

Since the populations of the different states remain constant in this weak probe approximation,

$$\rho_{jj;N}^{wp}(t) \equiv \rho_{jj;0}^{wp}\,\delta_{N,0} = \rho_{jj}^{wp}(t=0). \tag{3.8}$$

The steady state solution of equation (3.7) can be obtained by setting the time derivatives to zero and solving the resultant system of linear equations, that is,

$$[\omega^{(j)} + \omega_p - \omega^{(i)} + i\Gamma^{(i)}/2 + N\omega_c]\rho_{ij;N}^{wp}$$
$$+ \frac{1}{2}\sum_{l\in B}[\Omega_{c;il}\rho_{lj;N-1}^{wp} + \Omega_{c;li}^{*}\rho_{lj;N+1}^{wp}] = -\frac{1}{2}\,\Omega_{p;ij}\rho_{jj;0}^{wp}\delta_{N,0}, \tag{3.9}$$

where $i \in B$, $j \in A$, $N_{min} \le N \le N_{max}$ and $\rho_{ij;N}^{wp} \equiv \rho_{ij;N}^{wp}(t \to \infty)$. Calculating the absorption spectrum in the weak probe limit thus reduces to solving this system of equations for each state of group A and obtaining the absorption coefficient from equation (2.31) with $\rho_{ij;0}^{rw}(t \to \infty)$ replaced by $\rho_{ij;0}^{wp}$ — i.e. from the equation

$$\chi(\omega_p, \omega_c, \mathcal{E}_c) = \frac{N_d}{\epsilon_0 \mathcal{E}_p}\sum_{i\in B}\sum_{j\in A}\langle j|\hat{D}_z|i\rangle\rho_{ij;N=0}^{wp}. \tag{3.10}$$

The fact that $\Omega_{p;ij} \propto \mathcal{E}_p$ implies that $\rho_{ij;N=0}^{wp} \propto \mathcal{E}_p$ and therefore the susceptibility does not depend on $\mathcal{E}_p$ in this approximation.

We note that only the total dephasing rates $\Gamma^{(i)}/2$ appear in this formulation of the optical Bloch equations, rather than the individual relaxation rates Γ_{ij}. Contrary to equation (2.15), equation (3.9) therefore applies even to cases where the states of group B decay to other states than those of group A, which makes it well suited for describing systems with complex de-excitation pathways.

We also note that the equations forming this system decouple from each other in the absence of the coupling field (i.e. for $\mathcal{E}_c = 0$); equation (3.9) then yields

$$\rho_{ij;0}^{wp} = -\frac{\Omega_{p;ij}/2}{\omega^{(j)} + \omega_p - \omega^{(i)} + i\Gamma^{(i)}/2}\,\rho_{jj;0}^{wp}, \tag{3.11}$$

in agreement with well known theory — see, e.g. [49].

(b) Complex energies

Equation (3.9) was derived from the Lindblad master equation in the above, starting from the Hermitian Hamiltonian $\hat{H}(t)$ of equation (2.9). However, it is easy to see that the same result would also be obtained, in the weak probe approximation, if the density operator was instead calculated by solving the equation

$$\frac{d\hat{\rho}}{dt} = -\frac{i}{\hbar}\,[\hat{H}', \hat{\rho}\,], \tag{3.12}$$

with $\hat{H}'(t)$ taken to be the non-Hermitian Hamiltonian

$$\hat{H}'(t) = \sum_{i\in A}\hbar\omega^{(i)}|i\rangle\langle i| + \sum_{i\in B}\hbar\left(\omega^{(i)} - i\Gamma^{(i)}/2\right)|i\rangle\langle i|$$
$$- \frac{\hbar}{2}\sum_{i,j}\left\{[\Omega_{p;ij}\exp(-i\omega_p t) + \Omega_{c;ij}\exp(-i\omega_c t)]\,|i\rangle\langle j| + \text{h.c.}\right\}. \tag{3.13}$$

In this alternative approach, the states of group B are given a phenomenological width $\hbar\Gamma^{(i)}$ and the steady state of the system is derived solely from the effective Hamiltonian $\hat{H}'(t)$ by integrating the von Neumann equation. The two approaches are equivalent in the weak probe approximation in so far as they predict the same results. However, they would generally lead to different results beyond that approximation, in which case energy relaxation needs to be taken into account through the Lindblad master equation rather than through complex energies.

(c) Dressed states

Equation (3.9) has a close similarity with the equation defining the dressed states of the system in the absence of the probe field, as we now discuss. By dressed states, we mean, here, the quasistationary solutions of the equation

$$\left[i\hbar\frac{\mathrm{d}}{\mathrm{d}t} - \sum_{i\in B} \hbar\left(\omega^{(i)} - i\Gamma^{(i)}/2\right)|i\rangle\langle i| + \mathbf{E}_{\mathrm{c}}(t)\cdot\hat{\mathbf{D}} \right]|\Psi(t)\rangle = 0, \tag{3.14}$$

where $\hat{\mathbf{D}}$ is the dipole operator. The dressed states in question are solutions of the Floquet form,

$$|\Psi^{(q)}(t)\rangle = \exp(-i\epsilon^{(q)}t/\hbar)|\Phi^{(q)}(t)\rangle, \tag{3.15}$$

where $\epsilon^{(q)}$ is a constant and the ket vector $|\Phi^{(q)}(t)\rangle$ is time-periodic with period $2\pi/\omega_{\mathrm{c}}$. We expand the latter in a Fourier series with time-independent harmonic components $|\psi_N^{(q)}\rangle$ and write

$$|\Psi^{(q)}(t)\rangle = \exp(-i\epsilon^{(q)}t/\hbar)\sum_N \exp(-iN\omega_{\mathrm{c}}t)|\psi_N^{(q)}\rangle. \tag{3.16}$$

Since the field $\mathbf{E}_c(t)$ only couples states belonging to group B to other states of that group, we set

$$|\psi_N^{(q)}\rangle = \sum_{i\in B} a_{i;N}^{(q)}|i\rangle. \tag{3.17}$$

It is not difficult to show that the coefficients $a_{i;N}^{(q)}$ satisfy a system of equations similar (but not identical) to equation (3.9), i.e.

$$\left[\epsilon^{(q)} - \hbar\left(\omega^{(i)} - i\Gamma^{(i)}/2\right) + N\hbar\omega_{\mathrm{c}}\right] a_{i;N}^{(q)} + \frac{\hbar}{2}\sum_{l\in B}\left[\Omega_{\mathrm{c};il} a_{l;N-1}^{(q)} + \Omega_{\mathrm{c};li}^* a_{l;N+1}^{(q)}\right] = 0. \tag{3.18}$$

In matrix form,

$$\left[\epsilon^{(q)}\,\mathsf{I}_{\mathrm{Fl}} - \mathsf{F}\right]\mathsf{v}^{(q)} = 0, \tag{3.19}$$

where $\mathsf{v}^{(q)}$ is the column vector formed by the coefficients $a_{i;N}^{(q)}$, I_{Fl} is the $\mathcal{N}_{\mathrm{Fl}} \times \mathcal{N}_{\mathrm{Fl}}$ unit matrix with $\mathcal{N}_{\mathrm{Fl}} = (N_{\mathrm{max}} - N_{\mathrm{min}} + 1)\mathcal{N}_B$, where $\mathcal{N}_B$ is the number of states belonging to group B, and F is a $\mathcal{N}_{\mathrm{Fl}} \times \mathcal{N}_{\mathrm{Fl}}$ non-Hermitian matrix. This matrix represents the Floquet Hamiltonian and describes how the states of group B are coupled to each other by the coupling field beyond the rotating wave approximation.

How these dressed states relate to the solutions of equation (3.9) may be best brought out by recasting the latter in terms of the matrix F. For each state $j\in A$, we write equation (3.9) as

$$\left[(\omega^{(j)} + \omega_{\mathrm{p}})\,\mathsf{I}_{\mathrm{Fl}} - \mathsf{F}/\hbar\right]\mathsf{x}^{(j)} = \mathsf{b}^{(j)}, \tag{3.20}$$

where I_{Fl} and F are the matrices defined above (the same for all states j), $\mathsf{x}^{(j)}$ is the column vector formed by the coherences $\rho_{ij;N}^{\mathrm{wp}}$ and $\mathsf{b}^{(j)}$ is the column vector formed by the right-hand sides of equation (3.9). We will assume that F is not defective in view of the fact that this matrix would be Hermitian if the decay rates Γ_i were zero. The results outlined below do not apply if F is defective. The coherences derived from equation (3.26) would be incorrect and would differ from those obtained by solving equation (3.9) in this case.

Clearly, the eigenvalues of F are the complex quasienergies $\epsilon^{(q)}$ defined above and the right-hand side eigenvectors are the column vectors $v^{(q)}$:

$$F v^{(q)} = \epsilon^{(q)} v^{(q)}. \tag{3.21}$$

We denote the corresponding left-hand side eigenvectors by $u^{(q)}$ and define them as being the column vectors such that

$$u^{(q)\dagger} F = \epsilon^{(q)} u^{(q)\dagger}. \tag{3.22}$$

Let U and V be the matrices formed by the column vectors $u^{(q)}$ and $v^{(q)}$, respectively, with $u^{(q)}$ and $v^{(q)}$ normalised in such a way that $u^{(q)\dagger}v^{(q)} = 1$. Then $u^{(q)\dagger}v^{(q')} = \delta_{qq'}$ and $U^\dagger V = V U^\dagger = I_{Fl}$ [50]. Therefore

$$U^\dagger \left[(\omega^{(j)} + \omega_p) I_{Fl} - F/\hbar \right] V = \Lambda^{(j)} \tag{3.23}$$

where $\Lambda^{(j)}$ is the diagonal matrix of elements $(\omega^{(j)} + \omega_p - \epsilon^{(q)}/\hbar)\,\delta_{qq'}$. It follows from equation (3.20) that

$$U^\dagger \left[(\omega^{(j)} + \omega_p) I_{Fl} - F/\hbar \right] V U^\dagger x^{(j)} = U^\dagger b^{(j)}, \tag{3.24}$$

and therefore[2]

$$x^{(j)} = V [\Lambda^{(j)}]^{-1} U^\dagger b^{(j)} = \sum_q \frac{u^{(q)\dagger} b^{(j)}}{\omega^{(j)} + \omega_p - \epsilon^{(q)}/\hbar} v^{(q)}. \tag{3.25}$$

More explicitly,

$$\rho_{ij;N}^{wp} = \sum_q \frac{u^{(q)\dagger} b^{(j)}}{\omega^{(j)} + \omega_p - \epsilon^{(q)}/\hbar} \rho_{ij;N}^{(q)}, \tag{3.26}$$

where $\rho_{ij;N}^{(q)}$ is the component of the vector $v^{(q)}$ corresponding to the coherence $\rho_{ij;N}^{wp}$. Calculating the coherences in this way is completely equivalent to solving equation (3.9). However, this alternative formulation makes it possible to identify the contribution of the different dressed states to the susceptibility $\chi(\omega_p, \omega_c, \mathcal{E}_c)$. It is also advantageous in calculations of $\chi(\omega_p, \omega_c, \mathcal{E}_c)$ over a range of probe frequencies since the eigenvalues $\epsilon^{(q)}$, the eigenvectors $v^{(q)}$ and the inner products $u^{(q)\dagger}b^{(j)}$ do not depend on ω_p and can be calculated once and for all. In particular, this result makes it easier to average the susceptibility over a statistical distribution of values of ω_p, as may be required, e.g. for taking inhomogeneous broadening into account [55].

Finally, we note that these results must be corrected if the coherences ρ_{ij} also decay not only through energy relaxation but also through some pure dephasing mechanisms such as collisional broadening or phase fluctuation of the probe field. Denoting the corresponding additional dephasing rates by γ_{ij}, $\Gamma^{(i)}/2$ should then be replaced by $\Gamma^{(i)}/2 + \gamma_{ij}$ in equations (3.4), (3.7), (3.9) and (3.11) and $\omega^{(j)} + \omega_p - \epsilon^{(q)}/\hbar$ should be replaced by $\omega^{(j)} + \omega_p - \epsilon^{(q)}/\hbar + i\gamma_{ij}$ equations (3.25) and (3.26).

4. Numerical illustration

We now illustrate the theory developed in the previous section by numerical calculations for a simple toy model. An application to a much more complicated case is reported elsewhere [36]. The system we are considering here comprises only five states, namely, a single lower energy state (state 0, here the only element of group *A*) and four higher energy states (states 1, 2, 3 and 4, forming group *B*). As shown in figure 1*a*, state 0 is coupled to states 1 and 2 by the probe field while states 1 and 2 are coupled to states 3 and 4 by the coupling field. States 1 and 2 decay to state 0 only, whereas states 3 and 4 are assumed to have zero decay rates. The parameters of the model are largely arbitrary and do not correspond to any actual system. We assume a frequency of 1 GHz for the coupling field and, in most of the calculations, a frequency of 100 THz for the probe field (this frequency is varied around 100 THz in figure 2*b*). State 0 being the only member
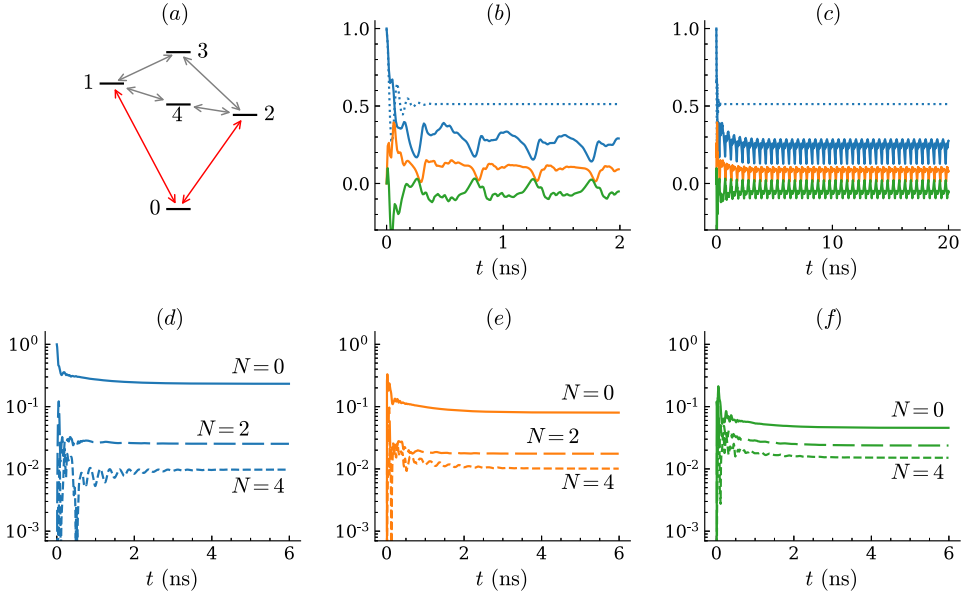
Figure 1. (*a*) The five-state system considered in §4: states 1 and 2 are addressed from state 0 by the probe field and coupled to states 3 and 4 by the coupling field. (*b*) and (*c*) Dotted blue curves: time evolution of $\rho_{00}^{rw}(t)$ in the absence of the coupling field. Solid curves, from top to bottom: time evolution of $\rho_{00}^{rw}(t)$ (solid blue curves), Im $\rho_{10}^{rw}(t)$ (solid orange curves) and Im $\rho_{20}^{rw}(t)$ (solid green curves) in the presence of the coupling field. (*d*) Time evolution of $|\text{Re } \rho_{00;N}^{rw}(t)|$ for $N = 0$ (solid curve), $N = 2$ (long-dashed curve) and $N = 4$ (short-dashed curve). (*e*) The same as (*d*) for $|\text{Im } \rho_{10;N}^{rw}(t)|$. (*f*) The same as (*d*) for $|\text{Im } \rho_{20;N}^{rw}(t)|$.
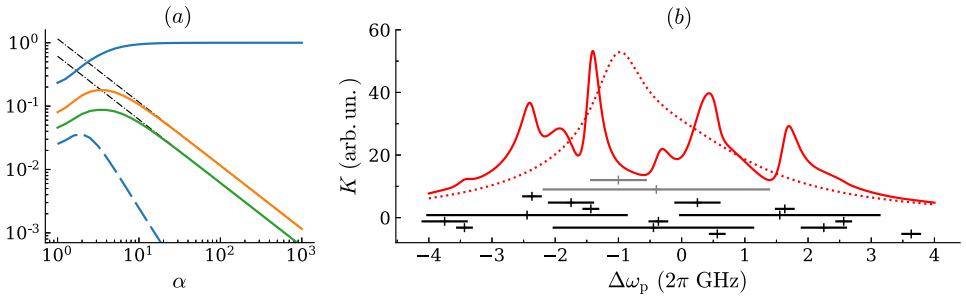
Figure 2. (*a*) From top to bottom, variation with the scaling parameter α of $\rho_{00;0}^{rw}(t)$ (solid blue curve), of $|\text{Im } \rho_{10;0}^{rw}(t)|$ (solid orange curve), of $|\text{Im } \rho_{20;0}^{rw}(t)|$ (solid green curve), and of $|\text{Re } \rho_{00;2}^{rw}(t)|$ (dashed blue curve), at $t = 200$ ns. The dash-dotted black lines show how the weak probe $|\text{Im } \rho_{10;0}^{wp}(t)|$ and $|\text{Im } \rho_{20;0}^{wp}(t)|$ vary for the same parameters. (*b*) The variation of the absorption coefficient with probe frequency in the presence of the coupling field (solid red curve and black markers) and in the absence of the coupling field (dotted red curve and grey markers). The markers refer to the energy and width of the dressed states contributing most to the absorption spectrum in the range of frequencies spanned by the figure: the real part of the quasienergy of each of these dressed states is identified by a vertical tick mark located at the corresponding value of $\Delta\omega_p^{(q)}$ and its decay width is indicated by a horizontal bar (see text).

of group A, we choose ω^{ref} to coincide with $\omega^{(0)}$ so that $\delta\omega^{(0)} = 0$. We set the detunings $\Delta_p^{(i)}$ and the Rabi frequencies $\Omega_{c;ij}$ to the values listed in table 1. We also assume that $\langle 0|\hat{D}_z|1\rangle = 2\langle 0|\hat{D}_z|2\rangle$. For consistency, we thus set $\Omega_{p;10} = 2\,\Omega_{p;20}$ and $\Gamma^{(1)} = 4\,\Gamma^{(2)}$. Specifically, we take $\Gamma_1 = 2\pi \times 3.6$ GHz, $\Gamma_2 = 2\pi \times 0.9$ GHz and, when obtaining the results shown in figure 1, $\Omega_{p;10} = 2\pi \times 10$ GHz and $\Omega_{p;20} = 2\pi \times 5$ GHz (other values of $\Omega_{p;10}$ and $\Omega_{p;20}$ are used in figure 2).

Table 1. Detunings and Rabi frequencies used in the examples, in units of 2π GHz.

examples	$\Delta_p^{(1)}$	$\Delta_p^{(2)}$	$\Delta_p^{(3)}$	$\Delta_p^{(4)}$	$\Omega_{c;13}$	$\Omega_{c;14}$	$\Omega_{c;23}$	$\Omega_{c;24}$
figures 1 and 2a	0.4	1.0	−0.2	0.8	9	11	6	9
figure 2b		variable			0.9	1.1	0.6	0.9

Table 2. Convergence of the solutions of equation (2.26) to the solutions of equation (2.18) for increasingly wide ranges of the values of N included in the calculation, for the system considered in figure 1. The relevant detunings and Rabi frequencies are listed in table 1.

$[N_{\min}, N_{\max}]$	$\rho_{00}^{\mathrm{rw}}(t = 20\,\mu s)$	$\mathrm{Im}\,\rho_{10}^{\mathrm{rw}}(t = 20\,\mu s)$	$\mathrm{Im}\,\rho_{20}^{\mathrm{rw}}(t = 20\,\mu s)$
$[-10, 10]$	0.2774771	0.0761685	−0.0615402
$[-20, 20]$	0.2759140	0.0797740	−0.0564471
$[-30, 30]$	0.2760659	0.0794110	−0.0568168
$[-40, 40]$	0.2753107	0.0794474	−0.0564466
$[-50, 50]$	0.2753153	0.0793790	−0.0565258
Eq. (18)	0.2753153	0.0793790	−0.0565258

How some of the populations and coherences vary in time for this set of parameters is shown in figure 1b–f. The time-dependent harmonic components $\rho_{ij;N}^{\mathrm{rw}}(t)$ were calculated by numerically integrating equation (2.26) and the density matrix by summing these harmonic components as per equation (2.30). The range of values of N used in the computation was wide enough that the results were not significantly affected by the truncation of the system (24) to a finite number of equations: we set $N_{\min} = -50$ and $N_{\max} = 50$. As listed in table 2, this choice ensured that the populations and coherences calculated from equations (2.26) and (2.30) matched those calculated from equation (2.18) to seven decimal places (a smaller range of values of N would be sufficient for weaker fields). Results calculated are also presented for the case of a zero coupling field (the dotted curves in figure 1b,c).

How the ground state population $\rho_{00}^{\mathrm{rw}}(t)$ and the imaginary parts of the coherences $\rho_{10}^{\mathrm{rw}}(t)$ and $\rho_{20}^{\mathrm{rw}}(t)$ vary immediately after the probe laser is turned on is shown in figure 1b and, over a longer time period, in figure 1c. In the absence of the coupling field (i.e. for $\Omega_{c;ij} \equiv 0$), the populations and coherences rapidly settle to constant values. However, they continue to oscillate markedly past the initial transients when the coupling field is strong. As shown by the solid curves, they settle into a state of periodic oscillation of period $4\pi/\omega$ when $t \to \infty$. By contrast, the harmonic components converge to constant values, reached asymptotically after a short phase of damped oscillations (figure 1d–f, no results are shown for $N = 1$ and 3 because $\rho_{00;N}^{\mathrm{rw}}(t)$, $\rho_{10;N}^{\mathrm{rw}}(t)$ and $\rho_{20;N}^{\mathrm{rw}}(t)$ are identically zero for odd values of N). One can also note the importance of the $N \neq 0$ harmonic components of the ground state population although this state does not directly interact with the coupling field in the present model. These harmonic components are responsible for the oscillation of $\rho_{00}^{\mathrm{rw}}(t)$. They arise from the indirect interaction of the ground state with the coupling field originating from its coupling to states 1 and 2 by the probe field.

The results shown in figure 1b–f refer to a relatively strong probe field. Convergence to the predictions of the weak probe approximation for decreasing values of $\mathcal{E}_p$ is illustrated by figure 2a, which shows results obtained by integrating equation (2.26) for values of $\Omega_{p;10}$ and $\Omega_{p;20}$ scaled by a factor $1/\alpha$: the probe field has the same strength as in figure 1b–f when $\alpha = 1$ but is weaker by a factor $1/\alpha$ when $\alpha > 1$. The calculation is done for a sufficiently large value of t (200 ns) that the harmonic components $\rho_{ij;N}^{\mathrm{rw}}(t)$ have become constant in time. As expected, and as can be seen from the figure, $\rho_{00;N=0}^{\mathrm{rw}}(t)$ tends to 1 and $\rho_{00;N\neq0}^{\mathrm{rw}}(t)$ tends to 0 when α increases. Moreover, $\rho_{10;0}^{\mathrm{rw}}(t)$

and $\rho^{\rm rw}_{20;0}(t)$ tend to the values predicted by equation (3.9), namely, $\rho^{\rm wp}_{10;0}$ and $\rho^{\rm wp}_{20;0}$. These values are proportional to $\mathcal{E}_p$, thus proportional to $1/\alpha$ here. (As can be deduced from a perturbative analysis and is apparent from the figure, $\rho^{\rm rw}_{00;2}(t) \propto 1/\alpha^2$.)

Finally, figure 2*b* illustrates the use of this formalism in the calculation and analysis of an absorption spectrum. The weak probe approximation is assumed to hold. As in part (*a*) of the same figure, the system is also taken be in the stationary state it relaxes into after the probe field has been turned on, past the initial transients. Here, however, $\omega_{\rm p}$ is varied: we set

$$\omega_{\rm p} = \omega_{\rm p0} + \Delta\omega_{\rm p}, \tag{4.1}$$

with $\omega_{\rm p0}/(2\pi) = 100$ THz. The detunings $\Delta^{(i)}_{\rm p}$ thus vary with $\Delta\omega_{\rm p}$ and have the same values as in figures 1 and 2*a* when $\Delta\omega_{\rm p} = 0$. The susceptibility and the absorption coefficient are calculated as functions of $\Delta\omega_{\rm p}$, by way of equations (3.10) and (2.7), respectively, with the products $N_{\rm d}\langle 0|\hat{D}_z|1\rangle/(\epsilon_0\mathcal{E}_{\rm p})$ and $N_{\rm d}\langle 0|\hat{D}_z|2\rangle/(\epsilon_0\mathcal{E}_{\rm p})$ set to values sufficiently low that $|\chi(\omega_{\rm p},\omega_{\rm c},\mathcal{E}_{\rm c})| \ll 1$.

The resulting absorption spectrum is plotted in figure 2*b*, both for the values of $\Omega_{{\rm c};ij}$ listed in table 1 (the solid curve) and for the case of a zero coupling field ($\Omega_{{\rm c};ij} \equiv 0$, the dotted curve). The relevant quasienergies are also indicated in the figure. As shown by equation (3.25), a dressed state of quasienergy $\epsilon^{(q)}$ contributes to the coherences $\rho^{\rm wp}_{i0}$ mostly for values of $\Delta\omega_{\rm p}$ in the range

$$\Delta\omega^{(q)}_{\rm p} - |{\rm Im}\,\epsilon^{(q)}/\hbar| \le \Delta\omega_{\rm p} \le \Delta\omega^{(q)}_{\rm p} + |{\rm Im}\,\epsilon^{(q)}/\hbar|, \tag{4.2}$$

where $\Delta\omega^{(q)}_{\rm p}$ is the value of $\Delta\omega_{\rm p}$ such that ${\rm Re}\,\epsilon^{(q)}/\hbar + \omega^{(0)} + \omega_{\rm p} = 0$. Accordingly, we identify the dressed states contributing most to the spectrum by tick marks positioned at the corresponding values of $\Delta\omega^{(q)}_{\rm p}$ and we represent their widths by bars of length $2\,|{\rm Im}\,\epsilon^{(q)}/\hbar|$. (The vertical position of these markers is arbitrary and has no physical meaning.)

The ground state interacts only with the bare states 1 and 2 when $\mathcal{E}_{\rm c} = 0$. Diagonalizing the matrix F, in that case, yields quasienergies either of the form $N\hbar\omega_{\rm c} - \hbar(\omega^{(1)} - i\Gamma^{(1)}/2)$ or of the form $N\hbar\omega_{\rm c} - \hbar(\omega^{(2)} - i\Gamma^{(2)}/2)$, $N = 0, \pm 1, \pm 2, \ldots$. Only the two solutions for which $\epsilon^{(q)}$ is either exactly $-\hbar(\omega^{(1)} - i\Gamma^{(1)}/2)$ or $-\hbar(\omega^{(2)} - i\Gamma^{(2)}/2)$ are relevant here, because, in the notation of equation (3.25), $\mathfrak{u}^{(q)}\mathfrak{b}^{(0)} = 0$ for the other solutions in the absence of the coupling field. The corresponding states overlap in energy within their respective decay width, as shown by the grey horizontal bars in the figure. The overlap results in a single non-Lorentzian peak in the absorption spectrum. This peak splits into multiple structures when the coupling field is on, for the relatively large values of $\Omega_{{\rm c};ij}$ assumed in the calculation. The structures originate from the interfering contributions of many dressed states. For clarity, only the 15 states contributing most to the spectrum in the range of frequencies considered are identified in the figure.

5. Conclusions

In conclusion, we have demonstrated how the well-known theory of absorption of a weak laser beam by a linear medium extends to cases where the medium is also addressed by a strong oscillating field, which couples states with significant decay widths. The Floquet formalism is the natural framework for modelling such systems. Calculating the absorption spectrum is particularly simple for weak probe beams. In the weak field limit, indeed, the relevant steady-state coherences can be obtained by solving a system of linear equations of reduced dimensionality, equation (3.9). Taking decay mechanisms into account in this context simply involves adding an imaginary part to the state energies, eliminating the need to solve the Lindblad master equation in its full complexity; however, these two formulations are mathematically equivalent. Moreover, the Floquet approach makes it possible to analyse the absorption spectrum in terms of individual contributions from dressed excited states induced by the coupling field, in the same way as it can be analyzed in terms of contributions of barely excited states in the absence of the coupling field. This Floquet analysis can greatly help elucidate the origin of resonance features modulating the probe absorption spectrum, as illustrated by figure 2*b*.

The methods described in this article have already been applied to the study of broad excitons coupled to each other by a strong microwave field [36]. More generally, they are applicable to any system driven by a strong oscillating field while being probed by a weak field, provided the rotating wave approximation and the Beer–Lambert law are valid for the latter.

Endnotes

[1]This transformation is unitary in the Hilbert space spanned by the basis of eigenvectors of the field-free Hamiltonian used throughout these calculations: $\hat{U}(t)\hat{U}^{\dagger}(t) = \hat{U}^{\dagger}(t)\hat{U}(t) = \sum_{i\in A}|i\rangle\langle i| + \sum_{j\in B}|j\rangle\langle j|$, which is the identity operator in that Hilbert space.

[2]This result can also be derived directly from the closure relation [50] $\sum_q v^{(q)}u^{(q)\dagger} = I_{Fl}$ and from the spectral decomposition of the operator $(\omega^{(j)} + \omega_p)I_{Fl} - F/\hbar$, i.e. $(\omega^{(j)} + \omega_p)I_{Fl} - F/\hbar = \sum_q(\omega^{(j)} + \omega_p - \epsilon^{(q)}/\hbar)v^{(q)}u^{(q)\dagger}$. It has a similar mathematical structure as expressions of the ionization rates derived from the spectral decomposition of the resolvent operator for atoms interacting with a weak probe beam in the presence of a strong static electric field [51,52] or a strong laser field [53,54].

References

1. Shirley JH. 1965 Solution of the Schrödinger equation with a Hamiltonian periodic in time. *Phys. Rev.* **138**, B979–B987. (doi:10.1103/physrev.138.b979)
2. Sambe H. 1973 Steady states and quasienergies of a quantum-mechanical system in an oscillating field. *Phys. Rev. A* **7**, 2203–2213. (doi:10.1103/physreva.7.2203)
3. Cohen-Tannoudji C, Reynaud S. 1977 Dressed-atom description of resonance fluorescence and absorption spectra of a multi-level atom in an intense laser beam. *J. Phys. B: At. Mol. Phys.* **10**, 345–363. (doi:10.1088/0022-3700/10/3/005)
4. Ho TS, Chu SI, Tietz JV. 1983 Semiclassical many-mode Floquet theory. *Chem. Phys. Lett.* **96**, 464–471. (doi:10.1016/0009-2614(83)80732-5)
5. Chu SI, Telnov DA. 2004 Beyond the Floquet theorem: generalized Floquet formalisms and quasienergy methods for atomic and molecular multiphoton processes in intense laser fields. *Phys. Rep.* **390**, 1–131. (doi:10.1016/j.physrep.2003.10.001)
6. Joachain CJ, Kylstra NJ, Potvliege RM. 2012 *Atoms in intense laser fields*. Cambridge, UK: Cambridge University Press. (doi:10.1017/CBO9780511993459)
7. Dörr M, Potvliege RM, Shakeshaft R. 1990 Multiphoton processes in an intense laser field: III. Resonant ionization of hydrogen by subpicosecond pulses. *Phys. Rev. A* **41**, 558–561. (doi:10.1103/physreva.41.558)
8. Day HC, Piraux B, Potvliege RM. 2000 Multistate non-Hermitian Floquet dynamics in short laser pulses. *Phys. Rev. A* **61**, 031402. (doi:10.1103/physreva.61.031402)
9. Potvliege RM, Vučić S. 2006 High-order above-threshold ionization of argon: plateau resonances and the Floquet quasienergy spectrum. *Phys. Rev. A* **74**, 023412. (doi:10.1103/physreva.74.023412)
10. Holthaus M. 2016 Floquet engineering with quasienergy bands of periodically driven optical lattices. *J. Phys. B At. Mol. Opt. Phys.* **49**, 013001. (doi:10.1088/0953-4075/49/1/013001)

11. Oka T, Kitamura S. 2019 Floquet engineering of quantum materials. *Annu. Rev. Condens. Matter Phys*. **10**, 387–408. (doi:10.1146/annurev-conmatphys-031218-013423)

12. Heugel TL, Biondi M, Zilberberg O, Chitra R. 2019 Quantum transducer using a parametric driven-dissipative phase transition. *Phys. Rev. Lett*. **123**, 173601. (doi:10.1103/physrevlett.123.173601)

13. Grimm A, Frattini NE, Puri S, Mundhada SO, Touzard S, Mirrahimi M, Girvin SM, Shankar S, Devoret MH. 2020 Stabilization and operation of a Kerr-cat qubit. *Nature* **584**, 205–209. (doi:10.1038/s41586-020-2587-z)

14. Wang X, Li HR, Li FL. 2020 Generating synthetic magnetism via Floquet engineering auxiliary qubits in phonon-cavity-based lattice. *New J. Phys*. **22**, 033037. (doi:10.1088/1367-2630/ab776e)

15. Geier S, Thaicharoen N, Hainaut C, Franz T, Salzinger A, Tebben A, Grimshandl D, Zürn G, Weidemüller M. 2021 Floquet Hamiltonian engineering of an isolated many-body spin system. *Science* **374**, 1149–1152. (doi:10.1126/science.abd9547)

16. Shan JY, Ye M, Chu H, Lee S, Park JG, Balents L, Hsieh D. 2021 Giant modulation of optical nonlinearity by Floquet engineering. *Nature* **600**, 235–239. (doi:10.1038/s41586-021-04051-8)

17. Weitenberg C, Simonet J. 2021 Tailoring quantum gases by Floquet engineering. *Nat. Phys*. **17**, 1342–1348. (doi:10.1038/s41567-021-01316-x)

18. Yin MJ, Lu XT, Li T, Xia JJ, Wang T, Zhang XF, Chang H. 2022 Floquet engineering Hz-level Rabi spectra in shallow optical lattice clock. *Phys. Rev. Lett*. **128**, 073603. (doi:10.1103/physrevlett.128.073603)

19. Blanco-Mas P, Creffield CE. 2023 Generating soliton trains through Floquet engineering. *Phys. Rev. A* **107**, 043310. (doi:10.1103/physreva.107.043310)

20. Bai SY, An JH. 2023 Floquet engineering to overcome no-go theorem of noisy quantum metrology. *Phys. Rev. Lett*. **131**, 050801. (doi:10.1103/physrevlett.131.050801)

21. Seibold K, Ameye O, Zilberberg O. 2024 Floquet expansion by counting pump photons. *Phys. Rev. Lett.* **134**, 060401. (doi:10.1103/PhysRevLett.134.060401)

22. Foot C. 2005 *Atomic physics*. Oxford, UK: Oxford University Press.

23. Chu SI, Reinhardt WP. 1977 Intense field multiphoton ionization via complex dressed states: application to the H atom. *Phys. Rev. Lett*. **39**, 1195–1198. (doi:10.1103/physrevlett.39.1195)

24. Potvliege RM, Shakeshaft R. 1989 Multiphoton processes in an intense laser field: harmonic generation and total ionization rates for atomic hydrogen. *Phys. Rev. A* **40**, 3061–3079. (doi:10.1103/physreva.40.3061)

25. Anderson DA, Schwarzkopf A, Miller SA, Thaicharoen N, Raithel G, Gordon JA, Holloway CL. 2014 Two-photon microwave transitions and strong-field effects in a room-temperature Rydberg-atom gas. *Phys. Rev. A* **90**, 043419. (doi:10.1103/physreva.90.043419)

26. Miller SA, Anderson DA, Raithel G. 2016 Radio-frequency-modulated Rydberg states in a vapor cell. *New J. Phys*. **18**, 053017. (doi:10.1088/1367-2630/18/5/053017)

27. Jiao Y, Hao L, Han X, Bai S, Raithel G, Zhao J, Jia S. 2017 Atom-based radio-frequency field calibration and polarization measurement using cesium nD_J Floquet states. *Phys. Rev. Appl*. **8**, 014028. (doi:10.1103/PhysRevApplied.8.014028)

28. Paradis E, Raithel G, Anderson DA. 2019 Atomic measurements of high-intensity VHF-band radio-frequency fields with a Rydberg vapor-cell detector. *Phys. Rev. A* **100**, 013420. (doi:10.1103/physreva.100.013420)

29. Rotunno AP, Berweger S, Prajapati N, Simons MT, Artusio-Glimpse AB, Holloway CL, Jayaseelan M, Potvliege RM, Adams CS. 2023 Detection of 3–300 MHz electric fields using Floquet sideband gaps by "Rabi matching" dressed Rydberg atoms. *J. Appl. Phys*. **134**, 134501. (doi:10.1063/5.0162101)

30. Wu S, Song W, Gao S, Chen Y, Zhu S, Li T. 2021 Floquet π mode engineering in non-Hermitian waveguide lattices. *Phys. Rev. Res.* **3**, 02311. (doi:10.1103/PhysRevResearch.3.023211)

31. Zhou L, Zhang DJ. 2023 Non-Hermitian Floquet topological matter—a review. *Entropy* **25**, 1401. (doi:10.3390/e25101401)

32. Moiseyev N. 1998 Quantum theory of resonances: calculating energies, widths and cross-sections by complex scaling. *Phys. Rep*. **302**, 212–293. (doi:10.1016/s0370-1573(98)00002-7)

33. Howland JS. 1974 Stationary scattering theory for time-dependent Hamiltonians. *Math. Ann*. **207**, 315–335. (doi:10.1007/bf01351346)

34. Yajima K. 1982 Resonances for the AC-Stark effect. *Commun. Math. Phys*. **87**, 331–352. (doi:10.1007/bf01206027)

35. Graffi S, Grecchi V, Silverstone HJ. 1985 Resonances and convergence of perturbation theory for N-body atomic systems in external AC-electric field. *Ann. Inst. H Poincaré* **42**, 215–234.

36. Brewin A, Gallagher LAP, Pritchett JD, Wong HQX, Potvliege RM, Clark SJ, Jones MPA. 2024 Microwave-optical spectroscopy of Rydberg excitons in the ultrastrong driving regime. *New J. Phys.* **26**, 113018. (doi:10.1088/1367-2630/ad8c74)

37. Ho TS, Wang K, Chu SI. 1986 Floquet-Liouville supermatrix approach: Time development of density-matrix operator and multiphoton resonance fluorescence spectra in intense laser fields. *Phys. Rev. A* **33**, 1798–1816. (doi:10.1103/physreva.33.1798)

38. Jacobs VL, Burke PG, Potvliege RM. 2014 Liouville-space R -matrix-Floquet description of atomic radiative processes involving autoionizing states in the presence of intense electro-magnetic fields. *J. Phys. B: At. Mol. Opt. Phys.* **47**, 025401. (doi:10.1088/0953-4075/47/2/025401)

39. Le Boité A. 2020 Theoretical methods for ultrastrong light–matter interactions. *Adv. Quantum Technol.* **3**, 1900140. (doi:10.1002/qute.201900140)

40. Chen H, Hu YM, Zhang W, Kurniawan MA, Shao Y, Chen X, Prem A, Dai X. 2024 Periodically driven open quantum systems: spectral properties and nonequilibrium steady states. *Phys. Rev. B* **109**, 184309. (doi:10.1103/physrevb.109.184309)

41. Wang K, Chu SI. 1987 Floquet–Liouville supermatrix approach. II. Intensity-dependent gen-eralized nonlinear optical susceptibilities. *J. Chem. Phys.* **86**, 3225–3238. (doi:10.1063/1.451981)

42. Nakano M, Yamaguchi K. 1994 Numerical Liouville approach: a calculation method for non-linear optical susceptibilities of N -state systems. *Phys. Rev. A* **50**, 2989–3004. (doi:10.1103/phys-reva.50.2989)

43. Nakano M, Yamaguchi K. 1995 Numerical Liouville approach: intensity-dependent transient linear and nonlinear optical susceptibilities. *Chem. Phys. Lett.* **234**, 323–329. (doi:10.1016/0009-2614(95)00058-c)

44. Sauvan P, Dalimier E. 2009 Floquet-Liouville approach for calculating Stark profiles in plas-mas in the presence of a strong oscillating field. *Phys. Rev. E* **79**, 036405. (doi:10.1103/phys-reve.79.036405)

45. Tanasittikosol M, Potvliege RM. 2012 Sidebands shifts and induced sidebands in rf-dressed Rydberg systems. *arxiv* (doi:10.48550/arXiv.1206.5951)

46. Gu B, Franco I. 2018 Optical absorption properties of laser-driven matter. *Phys. Rev. A* **98**, 063412. (doi:10.1103/physreva.98.063412)

47. Mishra C, Chakraborty A, Mishra SR. 2019 Spectral characteristics of a modified inverted-Y system beyond rotating wave approximation. *J. Phys. B At. Mol. Opt. Phys.* **52**, 095002. (doi:10.1088/1361-6455/ab1368)

48. Loudon R. 1983 *The quantum theory of light*, 2nd edn. Oxford, UK: Oxford University Press.

49. Zentile MA, Keaveney J, Weller L, Whiting DJ, Adams CS, Hughes IG. 2015 ElecSus: a pro-gram to calculate the electric susceptibility of an atomic ensemble. *Comput. Phys. Commun.* **189**, 162–174. (doi:10.1016/j.cpc.2014.11.023)

50. Wilkinson JH. 1965 *The algebraic eigenvalue problem*. Oxford, UK: Clarendon Press.

51. Alvarez G, Silverstone HJ. 1989 Resonance contributions to the photoionization spectrum of atomic hydrogen in an electric field. *Phys. Rev. Lett.* **63**, 1364–1367. (doi:10.1103/phys-revlett.63.1364)

52. Alvarez G, Silverstone HJ. 1989 Photoionization cross section: exact expansion over reso-nances and natural line shape. *Phys. Rev. A* **40**, 3690–3697. (doi:10.1103/physreva.40.3690)

53. Madajczyk JH, Pont M, Potvliege RM, Shakeshaft R, Taylor HS. 1992 Photoionization of atomic hydrogen dressed by a circularly polarized CO_2-laser field. *Phys. Rev. A* **45**, 4848–4854. (doi:10.1103/PhysRevA.45.4848)

54. Jaroń A, Mese E, Potvliege RM. 2000 Floquet analysis of laser-induced continuum structures. *J. Phys. B At. Mol. Opt. Phys.* **33**, 1487–1505. (doi:10.1088/0953-4075/33/8/302)

55. Potvliege RM, Wrathmall SA. 2025 CoOMBE: A suite of open-source programs for the inte-gration of the optical Bloch equations and Maxwell-Bloch equations. *Comput. Phys. Commun.* **306**, 109374. (doi:10.1016/j.cpc.2024.109374)

56. Potvliege R. 2025 dph0rmp/nonHermitian_Floquet_absorption: nonHermitian_Floquet_ab-sorption_v1.1 (1.1). Zenodo. (doi:10.5281/zenodo.14699497)